ACS APPLIED MATERIALS & INTERFACES

www.acsami.org

Research Article

Human Serum Phenylpyruvate Quantification Using Responsive 2D Photonic Crystal Hydrogels via Chemoselective Oxime Ligation: Progress toward Developing Phenylalanine-Sensing Elements

Kyeongwoo Jang, W. Seth Horne,* and Sanford A. Asher*

Cite This: *ACS Appl. Mater. Interfaces* 2020, 12, 39612−39619

Read Online

ACCESS | Metrics & More | Article Recommendations | Supporting Information

ABSTRACT: There is a need to develop at-home phenylalanine (Phe) test kits, analogous to home glucose meters, for phenylketonuria patients who must measure their blood Phe levels frequently to adjust their diet. Unfortunately, such test kits are not available yet because of the lack of simple and inexpensive Phe-sensing elements. With the goal of developing a Phe-sensing element, we fabricated two-dimensional photonic crystal (2DPC) hydrogels that quantify human serum phenylpyruvate (PhPY), which is the product of the reaction between Phe and the enzyme phenylalanine dehydrogenase. The PhPY-sensing hydrogels have oxyamine recognition groups that link PhPY to the hydrogel polymer network via chemoselective oxime ligation. This structural modification induces the hydrogel to swell, which then increases interparticle spacings within the embedded 2DPC. The PhPY-induced particle spacing changes are measured from light diffraction and used to quantify the PhPY concentrations. The estimated limit of detection of PhPY in human serum for a detection time of 30 min is 19 μM, which is comparable to the minimum blood Phe concentrations of healthy people. Besides the potential application for developing Phe-sensing elements, this new hydrogel sensing approach via chemoselective oxime ligation is generalizable to the development of other chemical sensors working in complex biological environments.

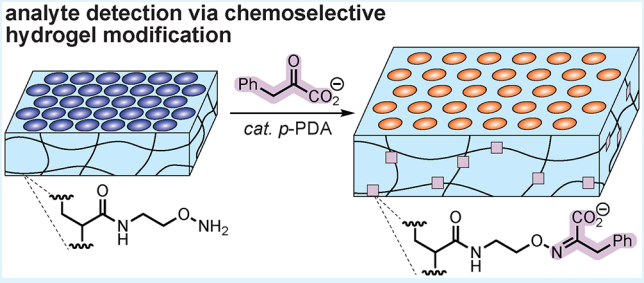

KEYWORDS: *responsive hydrogel, photonic crystal, oxime ligation, phenylalanine, phenylketonuria*

1. INTRODUCTION

Phenylketonuria (PKU) is a rare inborn error of metabolism that is caused by the deficiency of phenylalanine hydroxylase, which metabolizes phenylalanine (Phe) to tyrosine.[1] Untreated PKU patients have abnormally high blood Phe levels that can result in severe neurological disorders as well as symptoms including eczema, microcephaly, and seizures. Few medications, including sapropterin, have been developed to decrease Phe levels, and these are only effective for less than half of those with PKU.[2] The most common treatment for PKU is dietary, which involves the consumption of Phe-free medical formulas and reduced intake of natural protein. The treatment should be continued for life to maintain the blood Phe levels within 120−360 μM.[1] This requires PKU patients to frequently monitor their blood Phe levels and adjust their diet because excessively low Phe levels can also impede normal growth and development.[2]

To measure Phe levels, patients must take blood samples at home and mail these samples to clinics or laboratories or alternatively visit clinics to have blood samples taken. The typical turnaround time is 5−10 days, precluding real-time diet adjustment based on current conditions. Thus, there is a need to develop at-home Phe test kits analogous to home glucose meters because PKU patients would highly benefit from frequent feedback on their blood Phe levels as such data enable real-time diet adjustment.[2,3] Unfortunately, such test kits are not available yet.

Currently, three main clinical methods are used to measure blood Phe levels:[2] the Guthrie bacterial inhibition assay,[4] fluorometric analysis,[5,6] and tandem mass spectrometry.[7,8] Various laboratory techniques have also been developed to detect blood Phe utilizing high-performance liquid chromatography,[9,10] colorimetric assays,[11−13] electrochemistry,[14,15] chemiluminescence,[16,17] etc. None of these techniques has yet been successfully applied to develop at-home Phe test kits, largely because of the lack of simple and inexpensive Phe-sensing elements that can function in blood without the need for sophisticated instruments or trained personnel.

With the goal of developing a Phe-sensing element, we fabricated two-dimensional photonic crystal (2DPC) hydrogels

Received: May 13, 2020
Accepted: August 5, 2020
Published: August 5, 2020

capable of chemoselectively detecting phenylpyruvate (PhPY), which is the product of the reaction between Phe and the enzyme phenylalanine dehydrogenase (PheDH). The responsive 2DPC hydrogels, made of inexpensive materials, contain oxyamine functional groups that serve as molecular recognition agents. These hydrogel oxyamines chemoselectively react with the ketone in PhPY and covalently link PhPY to the hydrogel. This hydrogel structural modification gives rise to osmotic pressures, which cause hydrogel volume increases in response to increased concentrations of PhPY. The PhPY-induced volume changes are measured by light diffraction from the embedded 2DPCs, providing simple visible readouts that are used to quantify PhPY concentrations. The estimated limit of detection (LoD) of PhPY in human serum for a detection time of 30 min is 19 μM, which is comparable to the minimum blood Phe concentrations of healthy people. This proof-of-concept study demonstrates the capability of PhPY quantification in human serum via oxime formation which is widely used for bioconjugation applications.[18]

Although requiring further studies, our hypothesis is that the PhPY-sensing materials developed here could be applied to develop Phe-sensing elements by coupling with the enzyme PheDH. Prior studies have shown that the enzyme converts Phe to PhPY in whole blood and the concentrations of enzymatically produced PhPY are proportional to the Phe concentrations.[19,20] Thus, our PhPY-sensing hydrogels will be tested to quantify enzymatically produced PhPY to determine the concentration of Phe. These enzyme-coupled Phe-sensing elements could be utilized to develop at-home Phe test kits more inexpensively and efficiently than with existing Phe-sensing elements. The new hydrogel sensing approach via chemoselective oxime ligation appears generalizable and can be used to develop other chemical sensors, including those for a wide range of biomedically relevant targets.

2. EXPERIMENTAL SECTION

2.1. Materials. Acrylamide (AAm), acrylic acid (AAc), 2-hydroxy-4′-(2-hydroxyethoxy)-2-methylpropiophenone (Irgacure 2959), *N*,*N*′-methylenebisacrylamide (MBAAm), 1-propanol, anhydrous dimethylformamide (DMF), *p*-phenylenediamine (*p*-PDA), sodium phenylpyruvate (NaPhPY), L-phenylalanine (Phe), L-(−)-3-phenyllactic acid (PLA), phenylpropanoic acid (PPA), human serum (from human male AB plasma, U.S. origin, sterile-filtered), and an Amicon Ultra-15 Centrifugal Filter Unit (UFC 900308) were purchased from Sigma-Aldrich. *N*-(2-Bromoethyl)phthalimide, 1,8-diazabicyclo[5.4.0]undec-7-ene (DBU), anhydrous acetonitrile (MeCN), hydrazine hydrate, and *N*,*N*-diisopropylethylamine (DIPEA) were purchased from Acros Organics. Hydroxybenzotriazole hydrate (HOBT), 1-ethyl-3-(3-dimethylaminopropyl) carbodiimide hydrochloride (EDC), and *N*-Boc-hydroxylamine were purchased from Oakwood Products. Ethanol (200 proof) and hydrochloric acid were purchased from Decon Labs, Inc. and Thermo Fisher Scientific, respectively. All chemicals were used as received unless otherwise specified. AAc was purified by passing it through a glass pipette filled with alumina to remove the inhibitor. Human serum was centrifuged for 60 min at 5000*g* in Amicon Ultra-15 Centrifugal Filter Units to filter out serum proteins above 3 kDa. Ultrapure water (18.2 mΩ·cm) obtained from a Milli-Q Reference A+ was used for all experiments.

2.2. Characterization Techniques. *2.2.1. NMR.* ^{1}H and ^{13}C NMR spectra of the synthesized compounds (**1**−**3**) were recorded on Bruker AVANCE III 400 or 500 MHz spectrometers. Chemical shifts (δ) were reported relative to the residual $CHCl_3$ signal. High-resolution magic-angle spinning (HRMAS) ^{1}H NMR spectra of the hydrogels were recorded on a Bruker AVANCE 600 MHz wide-bore NMR spectrometer, equipped with a HRMAS accessory at a rotation rate of 4200 Hz at 300 K. For NMR spectroscopic studies, the hydrogels were prepared without 2DPCs. These hydrogels were thoroughly washed with Milli-Q water, freeze-dried, and placed in a 4 mm rotor. Approximately 40 μL of D_2O was added to 10 mg of each dry hydrogel. Chemical shifts (δ) were reported relative to the residual H_2O signal.

2.2.2. Mass Spectrometry. The high-resolution molecular masses of the synthesized compounds (**1**, **3**) were determined with a Thermo QExactive Instrument utilizing the positive electrospray ionization (ESI) technique at 70 K resolution.

2.2.3. Scanning Electron Microscopy. Periodic ordering of the 2DPC was monitored using a field emission scanning electron microscope (Zeiss Sigma 500) with an SE2 detector at an accelerating voltage of 3 kV after sputter-coating (PELCO SC-7, auto sputter coater) the samples with gold for 75 s at 30 mA.

2.3. Preparation of tert-Butyl(2-acrylamidoethoxy)-carbamate (TAC) via a Three-Step Sequence of Reactions. Synthesis of the TAC monomer (Scheme 1) proceeded as follows.

Scheme 1. Three-Step Sequence for the Preparation of TAC

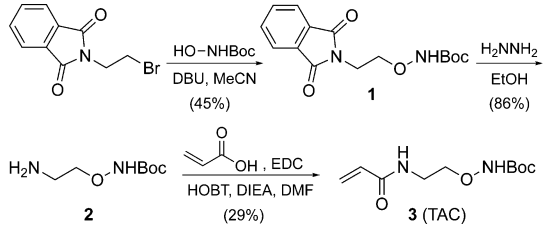

2.3.1. Synthesis of **1**.[21] *N*-Boc-hydroxylamine (10.10 g, 75.83 mmol, 1.0 equiv) and DBU (33.98 mL, 227.5 mmol, 3.0 equiv) were dissolved in dry MeCN (50 mL) and stirred for 10 min under N_2. The solution was cooled to 0 °C, and *N*-(2-bromoethyl)phthalimide (38.53 g, 151.7 mmol, 2 equiv) was added. The mixture was stirred for 2 h at 0 °C and 70 h at room temperature. The reaction mixture was diluted with 5% $NaHSO_4$ (30 mL), and the organic phase was extracted with ethyl acetate (EtOAc, 3 × 100 mL). The combined organic phases were brine washed, dried over $MgSO_4$, and concentrated by rotary evaporation. The crude material was purified by column chromatography (silica, hexane/EtOAc = 7:3) to yield product **1** (10.5 g, 34.2 mmol, 45%). R_f = 0.32 (hexane/EtOAc = 7:3). ^{1}H NMR ($CDCl_3$, 500 MHz): δ 1.47 (s, 9H), 4.00 (m, 4H), 7.73 (m, 2H), 7.76 (br, 1H), 7.86 (m, 2H). ^{13}C NMR ($CDCl_3$, 125 MHz): δ 28.4, 36.1, 73.2, 81.8, 123.6, 132.2, 134.3, 156.7, 168.8. HR-ESI-MS *m*/*z*: 307.13108 ([M + H]$^+$, calcd for $C_{15}H_{19}O_5N_2$, 307.12885).

2.3.2. Synthesis of **2**.[21,22] Hydrazine hydrate (4.53 mL, 93.3 mmol, 3 equiv) was added to a solution of **1** (9.54 g, 31.1 mmol, 1 equiv) and 100 mL of ethanol under N_2. The reaction mixture was stirred at 80 °C for 24 h. The solvent was removed by rotary evaporation, and 50 mL of cold dichloromethane was added to the residue. The amine product was extracted from the solid byproduct, phthalhydrazide, by stirring the mixture. The precipitated phthalhydrazide was filtered off, and the residue was washed with 50 mL of cold dichloromethane. Then, the combined filtrate and washings were mixed with 20 mL of saturated K_2CO_3 solution. The product was extracted with dichloromethane, and the organic layer was brine washed, dried over $MgSO_4$, and concentrated. The resulting crude product **2** (4.73 g, 26.8 mmol, 86%) was used without further purification. ^{1}H NMR ($CDCl_3$, 500 MHz): δ 1.48 (s, 9H), 2.99 (t, 2H, *J* = 9.8 Hz), 3.93 (t, 2H, *J* = 9.9 Hz).

2.3.3. Synthesis of **3** *(TAC).*[23] HOBT (0.7758 g, 5.067 mmol, 1.3 equiv) and **2** (4.73 g, 26.8 mmol, 1 equiv) were dissolved in dry DMF (50 mL) at 0 °C under Ar. After 10 min stirring, acrylic acid (2.39 mL, 34.9 mmol, 1.3 equiv) was added and the mixture was stirred for another 10 min. DIPEA (14.0 mL, 80.6 mmol, 3 equiv) was added, and the mixture was stirred for 15 min. EDC (7.72 g, 40.3 mmol, 1.5 equiv) was added, and the reaction mixture was stirred at room temperature for 20 h. The solution was diluted with 100 mL of water

https://dx.doi.org/10.1021/acsami.0c08787
ACS Appl. Mater. Interfaces 2020, 12, 39612−39619

and extracted using EtOAc. The organic layer was washed with 5% $NaHSO_4$(aq), 5% $NaHCO_3$(aq), water, and brine in sequence. The solution was dried over $MgSO_4$ and concentrated under reduced pressure. The crude product was purified using column chromatography (silica, hexane/EtOAc = 2:8) to yield product **3** (1.70 g, 7.77 mmol, 29%). ^{1}H NMR ($CDCl_3$, 400 MHz): δ 1.49 (s, 9H), 3.58 (q, 2H, J = 5.2 Hz), 3.91 (t, 2H, J = 4.8 Hz), 5.65 (dd, 1H, J = 10.1, 1.6 Hz), 6.18 (dd, 1H, J = 17.1, 10.2 Hz), 6.31 (dd, 1H, J = 17.0, 1.6 Hz), 7.09 (br, 1H), 7.34 (s, 1H). ^{13}C NMR ($CDCl_3$, 125 MHz): δ 28.3, 37.6, 76.0, 82.5, 126.3, 131.3, 158.0, 165.9. HR-ESI-MS m/z: 231.13476 ($[M + H]^+$, calcd for $C_{10}H_{19}O_4N_2$, 231.13393).

2.4. Preparation of 2DPC Hydrogels. First, negatively charged polystyrene (PS) spheres of a diameter of 1.23 μm were synthesized by dispersion polymerization. The detailed procedures were reported by Zhang et al.[24] These PS spheres (3 mL, 16% w/w in water) and 1 mL of 1-propanol were mixed. Then, using our previously reported needle-tip-flow technique (Figure 1a,b), a hexagonally close-packed PS 2DPC array was self-assembled on a water surface.[25] The self-assembled 2DPC array was transferred to a glass substrate (24 × 40 mm^2) and air dried (Figure 1c,d). Polymerizable monomer solutions were prepared following the composition listed in Table 1. The solutions were deoxygenated by injecting N_2 gas with a needle for 15 min (1 or 2 bubbles per second). After the initiator (8 μL of 33% w/v Irgacure 2959 in dimethyl sulfoxide) was added, the solutions were mildly vortexed for 15 s at 100 rpm. A 96 μL aliquot of the polymerizable solutions was layered on top of the preformed 2DPC array on a glass slide (Figure 1e). A cover slip was placed onto the 2DPC array to uniformly spread the polymerization solution. The free radical polymerization was then initiated by irradiating 365 nm UV light from a UVP Compact and Handheld UV Lamp (UVGL-55) for 15 min at room temperature (Figure 1f). The resulting cross-linked polymer chains incorporated the hexagonally ordered 2DPC array within the hydrogel network. Finally, the polymerized 2DPC hydrogel was peeled from the glass substrates and thoroughly washed with a phosphate-buffered saline solution (pH 7.2).

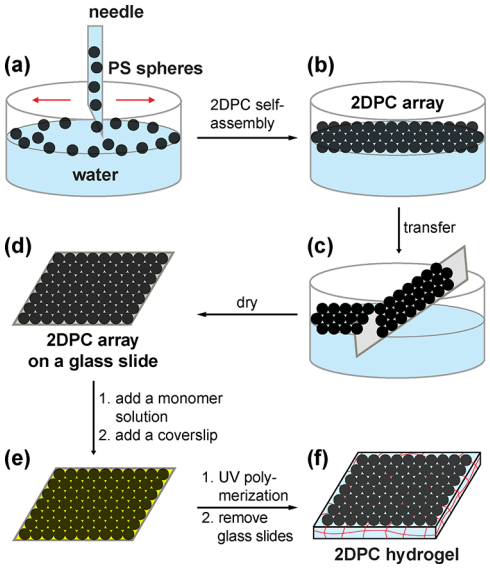

Figure 1. Method for fabricating 2DPC hydrogels. (a–d) First, a hexagonally close-packed PS 2DPC array was prepared on a glass substrate using the steps of our previously reported needle-tip-flow technique. (e) Polymerizable monomer solution was layered on top of a preformed 2DPC array on a glass slide. A cover slip sealed the solution, (f) after which a free radical polymerization was initiated by UV light. This cross-linked polymer incorporated the ordered 2DPC within the hydrogel network (2DPC hydrogel).

Table 1. Composition of Monomer Solutions Used in the Preparation of Hydrogel Samples

component	% (w/w)	mass (mg)
AAm	8	32
TAC	10	40
AAc	2	8
MBAAm	0.5	2
PG	45	180
H_2O	34.5	138
total	100	400

2.5. Hydrogel Boc Deprotection. After preparation of 2DPC hydrogels as described above, the Boc protecting groups in the polymer networks were removed by treatment with HCl. The as-prepared hydrogel was immersed in 12 mL of 1 M HCl and allowed to stand for 10 min. The HCl concentration was increased and decreased in increments to minimize osmotic shock to the hydrogel samples. The sequence of reagents added to the reaction were as follows: (1) 3 mL of 12 M HCl (final concentration 3 M HCl), (2) 5 mL of 12 M HCl (final concentration 5 M HCl), (3) 16 mL of water (final concentration 3 M HCl), and (4) 72 mL of water (final concentration 1 M HCl). The reaction was allowed to stand for 10 min after each addition. After the above sequence of steps, Boc-deprotected hydrogels were soaked in 100 mM acetate buffer (pH 5.5) overnight, cut into 5 × 5 mm^2 pieces with a razor blade, and stored in 100 mM acetate buffer (pH 5.5). The thickness of PhPY sense-ready hydrogels was estimated to be 145 μm.

2.6. 2DPC Particle Spacing Measurements. PhPY-induced hydrogel volume changes were monitored by measuring the 2DPC particle spacing, d, from the Debye diffraction ring diameters (Figure 2).[26] Hexagonally ordered 2DPCs diffract light according to the Bragg

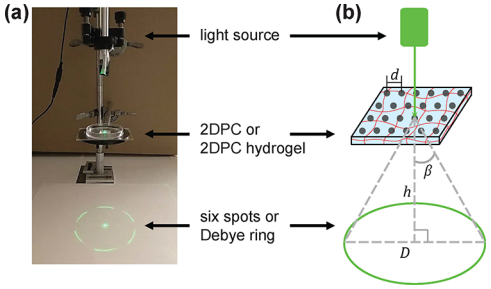

Figure 2. Debye ring diffraction measurement. A 5 × 5 mm^2 piece of the 2DPC hydrogels was placed parallel to a white screen below. (a) Experimental setup and (b) schematic diagram depicting the diffraction of the 2DPC hydrogel illuminated by 532 nm light from a laser pointer at normal incidence.

diffraction condition of eq 1, where m is the diffraction order, λ is the wavelength of the incident light, d is the spacing between each particle of the 2DPC, α is the incident angle of the light, and β is the diffracted angle of the light.

$$m\lambda = \frac{\sqrt{3}}{2} d(\sin\alpha + \sin\beta) \quad (1)$$

When 2DPCs or 2DPC hydrogels are irradiated using a 532 nm green laser pointer along the array normal (α = 0°), eq 1 reduces to

$$d = \frac{2(532\ \text{nm})}{\sqrt{3}\ \sin\beta} \quad (2)$$

For a perfectly ordered 2DPC, the light is strongly forward-diffracted at an angle β, producing six bright diffraction spots.[27] In our case where the sample is microcrystalline, consisting of numerous small rotationally disordered crystals, the diffraction formed a Debye ring on the screen below (Figure 2a). Equation 3 relates D, h, and β,

https://dx.doi.org/10.1021/acsami.0c08787
ACS Appl. Mater. Interfaces 2020, 12, 39612–39619

Scheme 2. Hydrogel PhPY-Sensing Chemistry

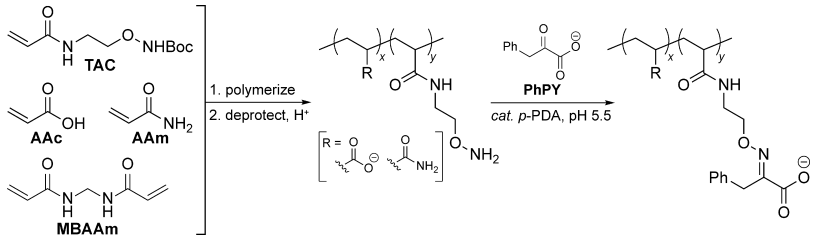

where D is the diameter of the Debye ring and h is the distance between the 2DPC plane and the bottom white paper (Figure 2b).

$$\beta = \tan^{-1}\frac{D}{2h} \tag{3}$$

Combining eqs 2 and 3 gives eq 4.

$$d = \frac{2(532\text{ nm})}{\sqrt{3}\,\sin\left(\tan^{-1}\frac{D}{2h}\right)} \tag{4}$$

h is typically fixed at 15 cm. Thus, the particle spacing d was calculated by measuring only D. To determine d of each sample, we measured nine different D's from three different positions within the same hydrogel sample and averaged them.

2.7. PhPY-Sensing in Buffer Solutions. For each reaction, a 5 × 5 mm^2 hydrogel was placed in a 10 mL solution of 100 mM acetate buffer (pH 5.5) containing 100 mM *p*-PDA. The hydrogel was equilibrated in the solution for 10 min, and the initial particle spacing was measured. A small aliquot of 100 mM of NaPhPY solution was added to initiate the PhPY-sensing reaction. For the first set of samples, the 2DPC particle spacings were measured every 5 min for 1 h. For the second set of samples, the reaction vials were mounted in a vortex mixer and agitated at 500 rpm. After the PhPY reaction proceeded for 30 min, the 2DPC particle spacings were measured again.

2.8. PhPY Sensing in Human Serum. The hydrogels (5 × 5 mm^2 pieces) were washed with 10 mM of acetate buffer solutions (pH 5.7) overnight. After the particle spacings were measured, each hydrogel was transferred to 10 mL of protein-removed human serum containing 500 mM *p*-PDA (pH 5.2, HCl was added to adjust the pH). A small aliquot of 100 mM of NaPhPY solution was added to each serum solution. The reaction vials were mounted in a vortex mixer and agitated at 500 rpm. After the PhPY reaction proceeded for 30 min, the hydrogels were thoroughly washed with 10 mM acetate buffer (pH 5.7) for 30 min, replacing the washing buffer every 10 min. Then, the 2DPC particle spacings were measured again.

3. RESULTS AND DISCUSSION

3.1. PhPY-Sensing Motif Using Responsive Hydrogels Containing 2DPC and Oxyamine Recognition Groups. Scheme 2 shows the hydrogel network and its PhPY-sensing chemistry. The copolymer structures shown are simplified representations of cross-linked networks. During polymerization, the newly synthesized monomer TAC was Boc-protected to mask the oxyamine nucleophilicity that could cause unwanted side reactions. Postpolymerization deprotection removed the Boc groups and released the free oxyamine groups, serving as PhPY recognition agents. Additionally, AAc and AAm monomers were copolymerized with TAC to increase the hydrophilicity of the resulting hydrogels.

Our design of the sensor was based on the hypothesis that the formation of oxime bonds between the PhPY carbonyl groups and the hydrogel oxyamine groups would serve as the basis for PhPY sensing. We employed the catalyst *p*-PDA to increase the oxime reaction rate in order to reduce the PhPY detection time. While oxime ligation is slow between pH 5 and 7 without a catalyst,[28,29] *p*-PDA increases the reaction rates 50- to 120-fold.[30−32]

The covalent attachment of PhPY changes the hydrogel composition, which causes the hydrogel volume to swell (Figure 3). The addition of PhPY carboxylates makes the hydrogel more hydrophilic and also localizes counterions. These characteristics generate a reaction-induced osmotic pressure, Π, in the hydrogel. The resulting change in Π causes the hydrogel volume to increase until the system reaches an equilibrium, where the osmotic pressure is uniform in both the hydrogel and the surrounding solution reservoir.[33,34] Furthermore, the hydrogel swelling increases the embedded 2DPC particle spacing, which is directly proportional to the PhPY concentration.

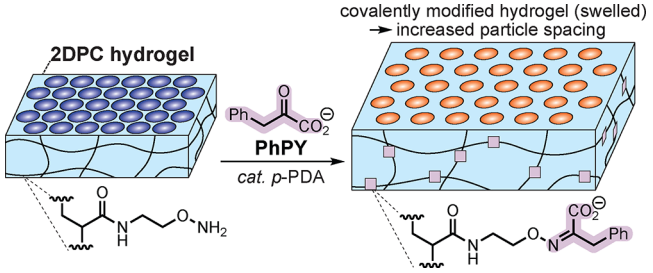

Figure 3. Schematic diagram of the PhPY-sensing hydrogel. The covalent attachment of PhPY changes the hydrogel composition, which causes the hydrogel to swell. The swelling increases the embedded 2DPC particle spacing in proportion to the PhPY concentration.

3.2. Characterizations of PhPY-Sensing Hydrogels. Figure 4a shows a scanning electron microscopy (SEM) image of the hexagonally close-packed PS 2DPC, which diffracts light according to the Bragg diffraction condition. The subsequent polymerization incorporated the 2DPC into the newly formed

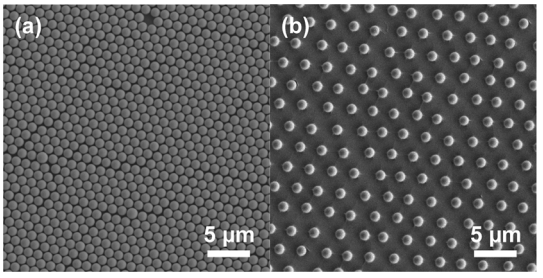

Figure 4. (a) SEM image of the hexagonally close-packed 2DPC consisting of PS particles of a diameter of 1.23 μm. (b) SEM image of the non-close-packed 2DPC embedded in the swollen hydrogel. As the hydrogel swelled, the array particle spacing homogeneously increased, maintaining the hexagonal ordering.

https://dx.doi.org/10.1021/acsami.0c08787
ACS Appl. Mater. Interfaces 2020, 12, 39612−39619

cross-linked polymer network. As the hydrogel swelled, the spacing of the embedded particles increased homogeneously, and the PS particles formed a non-close-packed 2DPC (Figure 4b). The hexagonal ordering of the embedded array was retained, which enabled the sensitive monitoring of the hydrogel volume change by measuring the 2DPC light diffraction. To prevent the non-close-packed particles from collapsing during the drying process, swollen 2DPC hydrogels were sandwiched between two glass substrates and dried in a desiccator before being sputter-coated.

NMR spectroscopy was used to characterize the PhPY-sensing hydrogels. Because of the reduced mobility of the individual backbone chains in the cross-linked polymer network, solution NMR spectra of most hydrogels show significant line broadening.[35,36] To improve the spectral resolution, a smaller amount (0.1% w/w) of the cross-linker (MBAAm) was used to prepare the hydrogels, and the magic-angle spinning (MAS) technique was employed.[37,38]

Figure 5a shows the water-suppressed ^{1}H NMR spectrum of the hydrogel before treatment with PhPY. The two sets of

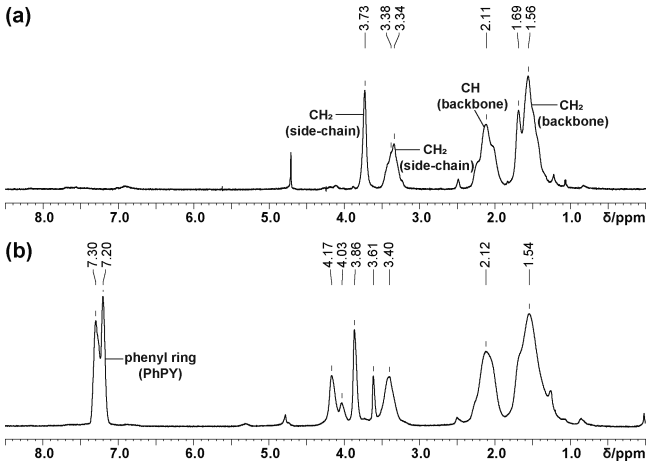

Figure 5. HRMAS ^{1}H NMR spectra of hydrogels (a) before and (b) after sensing PhPY. The new phenyl ring protons at δ = 7.2−7.3 demonstrate the attachment of PhPY to the hydrogel. The residual water signal at δ = 4.7 was suppressed by presaturation.

signals around δ = 1.56 and 2.11 ppm correspond to the polymer backbone CH_2 and CH groups, respectively. The other two sets of signals around δ = 3.34 and 3.73 ppm correspond to the side-chain CH_2 groups of TAC monomers. Before sensing PhPY, no proton peaks were observed at δ > 4 ppm (except the residual water signal). However, after sensing PhPY, new peaks were observed at δ = 7.2−7.3 ppm (Figure 5b), which correspond to the phenyl ring groups of the attached PhPY. The integrated areas of the phenyl protons at δ = 7.2 ppm and the polymer backbone protons at δ = 1.54 and 2.12 ppm roughly correspond to the hydrogel monomer composition. The NMR data obtained clearly demonstrate the covalent attachment of PhPY to the hydrogels.

3.3. PhPY Recognitions in Buffer Solutions. The PhPY-induced hydrogel swelling was monitored by measuring the embedded 2DPC particle spacings. First, each 5 × 5 mm^2 piece of the hydrogel was placed in a solution of acetate buffer (pH 5.5) containing 100 mM of *p*-PDA, and the initial particle spacing was measured. The average was 1740 nm (Figure 6a where time = 0 min), which is a 45% increase over the individual PS sphere diameter of 1.23 μm. This means that the

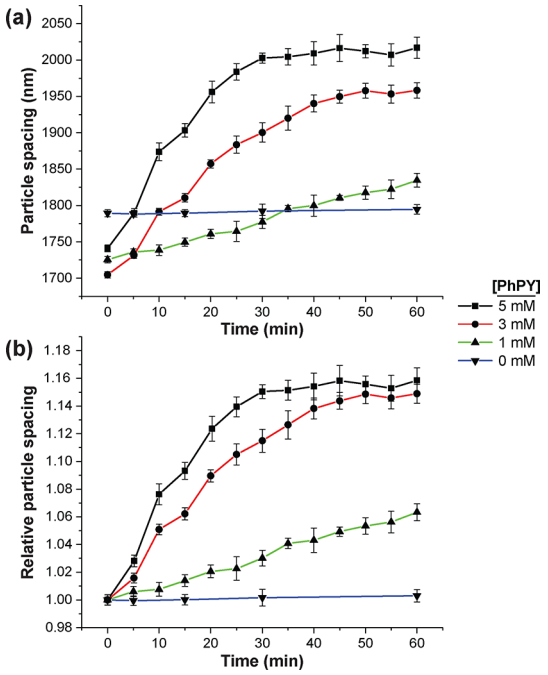

Figure 6. (a) Monitoring of the 2DPC particle spacing during PhPY-sensing reactions. *p*-PDA (100 mM) was employed in each reaction. (b) RPS was calculated and plotted to normalize the variance in the initial 2DPC particle spacings across the different hydrogel samples. Error bars represent standard deviations (n = 3).

hydrogel volumes were already swollen even before detecting PhPY, which is attributed to the presence of hydrophilic monomers. These PhPY-sensing hydrogels were mechanically robust and easy to handle.

Next, a different aliquot of 100 mM of NaPhPY solution was added to each hydrogel sample to initiate the PhPY-sensing reaction, and the particle spacing was measured every 5 min (Figure 6a). The hydrogels underwent larger particle spacing increases (or volume swellings) with faster reaction rates at higher PhPY concentrations. For example, 5 mM PhPY increased the particle spacing by 260 nm in 30 min, while 1 mM PhPY increased the particle spacing by only 110 nm in 1 h. The reason for this difference is that the magnitude of the swelling is proportional to the analyte concentration because the higher the PhPY concentration, the more PhPY molecules are attached to the hydrogels, generating a higher Π. In addition, the PhPY molecules are more likely to diffuse into the hydrogel network at higher PhPY concentrations, resulting in faster reaction rates. If no PhPY was present (0 mM), the particle spacings remained constant, showing that the hydrogel volume swellings were induced by the PhPY reactions.

Although the relative standard deviation is only 2%, the initial particle spacings varied across the different hydrogel samples, which makes it more difficult to analyze the data. To circumvent this issue, the individual particle spacing curve was scaled, and the relative particle spacing (RPS) curves were plotted instead (Figure 6b). For instance, all of the particle spacing data points in the 5 mM PhPY curve of Figure 6a were divided by the curve initial particle spacing, 1741 nm. The relative standard deviation of each data point was also calculated following the propagation of uncertainty. Then, the initial RPS value, where time = 0 min, always becomes 1, and the remaining data points show their relative changes compared with the initial point. The other particle spacing

https://dx.doi.org/10.1021/acsami.0c08787
ACS Appl. Mater. Interfaces 2020, 12, 39612−39619

curves were calculated in the same way. As a result, all of the RPS curves have the same initial value, which enables the different curves from various samples to be compared without bias. Thus, only RPS curves, calculated from the raw particle spacing curves, are discussed in the following results.

Figure 7 shows data supporting the chemoselectivity of the PhPY-sensing reaction. While PhPY induced a significant RPS increase, changes were negligible when testing close structural analogues: Phe, PLA, and PPA. This shows that the ketone group is vital and supports the hypothesis that the formation of an oxime with the hydrogel gives rise to the observed swelling. As an additional control, hydrogels lacking oxyamine groups were prepared by replacing TAC monomers with AAm. The RPS of these nonfunctional hydrogels did not increase after the incubation in PhPY. Thus, only when the hydrogels had oxyamine groups and PhPY was present, the RPS increased.

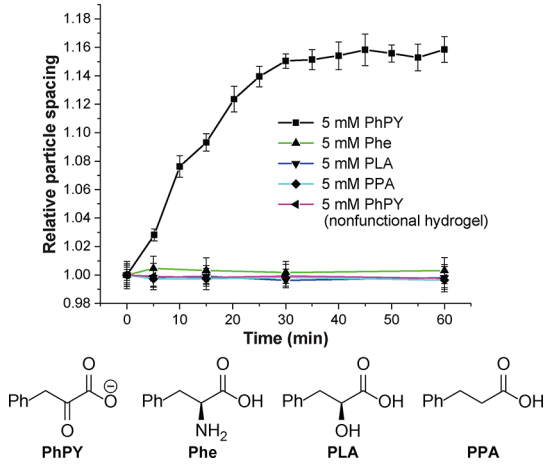

Figure 7. RPS curves demonstrating chemoselectivity of PhPY sensing. Only when the hydrogels had oxyamine groups and PhPY was present, the RPS increased. Error bars represent standard deviations (n = 3).

Figure 8 shows the concentration-dependent response of the sensor to PhPY at a fixed detection time of 30 min. To decrease the PhPY detection time, the reaction vials were agitated at 500 rpm using a vortex mixer. This agitation accelerated the diffusion rate of PhPY so that more PhPY molecules reached the oxyamines located inside the hydrogels, leading to larger and faster RPS increases in a shorter time. The effect of agitation can be clearly seen by comparing Figure 6b with Figure 8 at T = 30 min and [PhPY] = 1 mM. The RPS was only 1.030 when no agitation was employed (Figure 6b), but the RPS increased significantly to 1.125 when accompanied by agitation (Figure 8). Under these detection conditions, the LoD, estimated from the linear fit, was 93 μM (3*SD of y-intercept/slope).

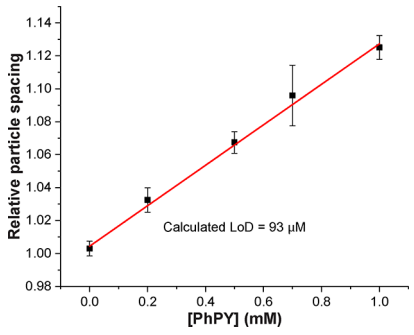

Figure 8. Quantification of PhPY for a detection time of 30 min. To decrease the detection time, the reaction vials were agitated at 500 rpm using a vortex mixer. The RPS at 0.7 mM PhPY had a much larger standard deviation compared to the other data points. The large standard deviation is potentially attributed to the relatively poorly ordered 2DPCs embedded into the corresponding hydrogel samples. The red line shows a linear fit (adjusted R-squared = 0.9968). Error bars represent standard deviations (n = 3).

3.4. PhPY Recognitions in Human Serum. The PhPY-sensing hydrogels were also tested in more complex biological milieu, human serum. Based on the preliminary results, we removed serum proteins to minimize interference. As in the previous experiments, we initially used a 100 mM concentration of p-PDA. However, because p-PDA showed a substantially lower solubility at physiological pH, it was necessary to add a relatively large amount of HCl to lower the pH and completely dissolve p-PDA. As a result, serum solutions containing 100 mM of p-PDA had much higher ionic strength than acetate buffer solutions containing the same concentration of p-PDA. This increased ionic strength of the serum solution screened the negative charges, which were attached to the hydrogels after detecting PhPY, thus minimizing Π and the hydrogel volume increase.

To avoid the ionic strength issue and increase the sensor responsivity, the hydrogels were washed with acetate buffer solutions with a low ionic strength of 10 mM before and after detecting PhPY. In this case, the ionic strength of the serum solution did not affect the particle spacing measurements, and the hydrogels showed larger volume changes after detecting PhPY. Further, 500 mM of p-PDA, much higher than 100 mM, was employed for PhPY sensing to maximize the oxime reaction rate.

Figure 9 shows the RPS data as a result of detecting various PhPY concentrations in protein-removed human serum (detection time = 30 min). The degree of increase in RPS was greater in the serum solutions than in the buffer solutions. This is because, as aforementioned, the p-PDA concentration was increased during the PhPY detection, and the hydrogels were washed with low-ionic-strength solutions after the reaction. For instance, where [PhPY] = 0.5 mM, the RPS in the buffer solutions was 1.067 (Figure 8); however, the RPS in the serum solutions was noticeably higher at 1.158 (Figure 9).

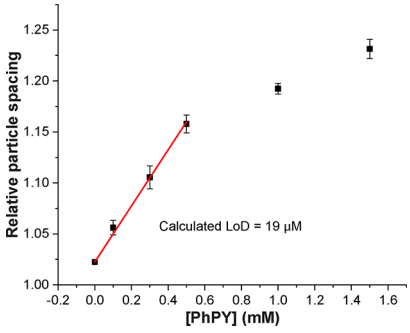

Figure 9. Quantification of PhPY in protein-removed human serum (detection time = 30 min). p-PDA (500 mM) was employed in each reaction. The red line shows a linear fit (adjusted R-squared = 0.9958). Error bars represent standard deviations (n = 3).

https://dx.doi.org/10.1021/acsami.0c08787
ACS Appl. Mater. Interfaces 2020, 12, 39612−39619

The red line shows a linear fit where [PhPY] ≤ 0.5 mM, and the LoD was estimated to be 19 μM (3*SD of *y*-intercept/slope). The change in the RPS began to level off when [PhPY] > 0.5 mM because the PhPY reaction gradually reached equilibrium. The results demonstrate that the 2DPC hydrogel sensor could be used to precisely determine the analyte concentrations in biological samples.

When [PhPY] = 0 mM in protein-removed human serum, the RPS was not 1 but slightly increased to 1.022. We hypothesize that this is due to the presence of other ketones or aldehydes that are normally present in blood at low levels. We do not anticipate that this would pose a problem in the potential future application of the reported material in the development of a blood Phe sensor by coupling the enzymatic conversion of Phe to PhPY with the PhPY-sensing hydrogels. The background RPS of untreated blood will be measured first without the enzymatic conversion and subtracted from the RPS determined after the enzymatic conversion.

The long-term stability of PhPY-sensing hydrogels was tested. After being stored in 100 mM acetate buffer solutions (pH 5.5) for 4 months at 4 °C, the hydrogel samples reacted with 0.5 mM of PhPY in protein-removed human serum as described above (n = 3). The aged samples showed a negligible difference in the RPS values compared with the data shown in Figure 9. This demonstrates that the hydrogels can be stored for a long time without losing their responsivity.

4. CONCLUSIONS

We have described here responsive 2DPC hydrogels for the chemoselective detection of PhPY, the reaction product of Phe with the enzyme PheDH. The PhPY-sensing hydrogels chemoselectively react with PhPY, leading to a change in hydrogel volume that is quantified by light diffraction from the embedded 2DPC. This covalent structural modification enables the hydrogels to be vigorously washed with a buffer solution of low ionic strength after PhPY reactions, resulting in greatly improved sensor responsivity. The estimated LoD of PhPY in protein-removed human serum for a detection time of 30 min is 19 μM, which is comparable to the minimum blood Phe concentrations of healthy people.

In future work, we plan to test our hypothesis that it is possible to couple the enzymatic conversion of Phe to PhPY with the newly reported PhPY-sensing hydrogels to develop a blood Phe sensor. The recognition of enzymatically produced PhPY would be able to quantify the Phe concentration because Phe produces a stoichiometric amount of PhPY from the reaction. Our ultimate goal is to incorporate this Phe sensor into an at-home test kit for PKU patients. Although these plans present technical challenges that must be addressed, with sufficient optimization, we propose that the sensor material presented here can be applied more inexpensively and efficiently than with existing Phe-sensing elements. This new hydrogel sensing approach via covalent oxime ligation, widely used in bioconjugation applications, can be generalized to develop other chemical sensors.

ASSOCIATED CONTENT

Supporting Information

The Supporting Information is available free of charge at https://pubs.acs.org/doi/10.1021/acsami.0c08787.

High-resolution mass spectrometry spectra of synthesized compounds and ^{1}H and ^{13}C NMR spectra of synthesized compounds (PDF)

AUTHOR INFORMATION

Corresponding Authors

W. Seth Horne − *Department of Chemistry, University of Pittsburgh, Pittsburgh, Pennsylvania 15260, United States;* orcid.org/0000-0003-2927-1739; Email: horne@pitt.edu

Sanford A. Asher − *Department of Chemistry, University of Pittsburgh, Pittsburgh, Pennsylvania 15260, United States;* orcid.org/0000-0003-1061-8747; Email: asher@pitt.edu

Author

Kyeongwoo Jang − *Department of Chemistry, University of Pittsburgh, Pittsburgh, Pennsylvania 15260, United States;* orcid.org/0000-0002-3665-2698

Complete contact information is available at: https://pubs.acs.org/10.1021/acsami.0c08787

Notes

The authors declare no competing financial interest.

ACKNOWLEDGMENTS

The authors acknowledge Krishnan Damodaran and Mike Delk for assistance in obtaining NMR spectra. The authors acknowledge the University of Pittsburgh and the Defense Threat Reduction Agency (grant no. HDTRA1-15-1-0038) for providing instrumentation and financial support.

REFERENCES

(1) Mitchell, J. J.; Trakadis, Y. J.; Scriver, C. R. Phenylalanine Hydroxylase Deficiency. *Genet. Med.* **2011**, *13*, 697−707.

(2) Camp, K. M.; Parisi, M. A.; Acosta, P. B.; Berry, G. T.; Bilder, D. A.; Blau, N.; Bodamer, O. A.; Brosco, J. P.; Brown, C. S.; Burlina, A. B.; Burton, B. K.; Chang, C. S.; Coates, P. M.; Cunningham, A. C.; Dobrowolski, S. F.; Ferguson, J. H.; Franklin, T. D.; Frazier, D. M.; Grange, D. K.; Greene, C. L.; Groft, S. C.; Harding, C. O.; Howell, R. R.; Huntington, K. L.; Hyatt-Knorr, H. D.; Jevaji, I. P.; Levy, H. L.; Lichter-Konecki, U.; Lindegren, M. L.; Lloyd-Puryear, M. A.; Matalon, K.; MacDonald, A.; McPheeters, M. L.; Mitchell, J. J.; Mofidi, S.; Moseley, K. D.; Mueller, C. M.; Mulberg, A. E.; Nerurkar, L. S.; Ogata, B. N.; Pariser, A. R.; Prasad, S.; Pridjian, G.; Rasmussen, S. A.; Reddy, U. M.; Rohr, F. J.; Singh, R. H.; Sirrs, S. M.; Stremer, S. E.; Tagle, D. A.; Thompson, S. M.; Urv, T. K.; Utz, J. R.; van Spronsen, F.; Vockley, J.; Waisbren, S. E.; Weglicki, L. S.; White, D. A.; Whitley, C. B.; Wilfond, B. S.; Yannicelli, S.; Young, J. M. Phenylketonuria Scientific Review Conference: State of the Science and Future Research Needs. *Mol. Genet. Metab.* **2014**, *112*, 87−122.

(3) American Academy of Pediatrics. National Institutes of Health Consensus Development Conference Statement: phenylketonuria: screening and management, October 16-18, 2000. *Pediatrics* **2001**, *108*, 972−982.

(4) Guthrie, R.; Susi, A. A Simple Phenylalanine Method for Detecting Phenylketonuria in Large Populations of Newborn Infants. *Pediatrics* **1963**, *32*, 338−343.

(5) Gerasimova, N. S.; Steklova, I. V.; Tuuminen, T. Fluorometric Method for Phenylalanine Microplate Assay Adapted for Phenylketonuria Screening. *Clin. Chem.* **1989**, *35*, 2112−2115.

(6) Mishra, D. R.; Darjee, S. M.; Bhatt, K. D.; Modi, K. M.; Jain, V. K. Calix Protected Gold Nanobeacon as Turn-Off Fluorescent Sensor for Phenylalanine. *J. Inclusion Phenom. Macrocyclic Chem.* **2015**, *82*, 425−436.

(7) Chace, D. H.; Sherwin, J. E.; Hillman, S. L.; Lorey, F.; Cunningham, G. C. Use of Phenylalanine-to-Tyrosine Ratio

Determined by Tandem Mass Spectrometry to Improve Newborn Screening for Phenylketonuria of Early Discharge Specimens Collected in the First 24 Hours. *Clin. Chem.* **1998**, *44*, 2405−2409.
(8) Corso, G.; Paglia, G.; Garofalo, D.; D'Apolito, O. Neutral Loss Analysis of Amino Acids by Desorption Electrospray Ionization Using an Unmodified Tandem Quadrupole Mass Spectrometer. *Rapid Commun. Mass Spectrom.* **2007**, *21*, 3777−3784.
(9) Roesel, R. A.; Blankenship, P. R.; Hommes, F. A. HPLC Assay of Phenylalanine and Tyrosine in Blood Spots on Filter Paper. *Clin. Chim. Acta* **1986**, *156*, 91−96.
(10) Neurauter, G.; Scholl-Bürgi, S.; Haara, A.; Geisler, S.; Mayersbach, P.; Schennach, H.; Fuchs, D. Simultaneous Measurement of Phenylalanine and Tyrosine by High Performance Liquid Chromatography (HPLC) with Fluorescence Detection. *Clin. Biochem.* **2013**, *46*, 1848−1851.
(11) De Silva, V.; Oldham, C. D.; May, S. W. L-Phenylalanine Concentration in Blood of Phenylketonuria Patients: A Modified Enzyme Colorimetric Assay Compared with Amino Acid Analysis, Tandem Mass Spectrometry, and HPLC Methods. *Clin. Chem. Lab. Med.* **2010**, *48*, 1271−1279.
(12) Thiessen, G.; Robinson, R.; De Los Reyes, K.; Monnat, R. J.; Fu, E. Conversion of a Laboratory-Based Test for Phenylalanine Detection to a Simple Paper-Based Format and Implications For PKU Screening in Low-Resource Settings. *Analyst* **2015**, *140*, 609−615.
(13) Robinson, R.; Wong, L.; Monnat, R.; Fu, E. Development of a Whole Blood Paper-Based Device for Phenylalanine Detection in the Context of PKU Therapy Monitoring. *Micromachines* **2016**, *7*, 28−37.
(14) Omidinia, E.; Shadjou, N.; Hasanzadeh, M. Immobilization of Phenylalanine-Dehydrogenase on Nano-Sized Polytaurine: A New Platform for Application of Nano-Polymeric Materials on Enzymatic Biosensing Technology. *Mater. Sci. Eng., C* **2014**, *42*, 368−373.
(15) Idili, A.; Parolo, C.; Ortega, G.; Plaxco, K. W. Calibration-Free Measurement of Phenylalanine Levels in the Blood Using an Electrochemical Aptamer-Based Sensor Suitable for Point-of-Care Applications. *ACS Sens.* **2019**, *4*, 3227−3233.
(16) Qiu, H.; Xi, Y.; Lu, F.; Fan, L.; Luo, C. Determination of L-Phenylalanine On-Line Based on Molecularly Imprinted Polymeric Microspheres and Flow Injection Chemiluminescence. *Spectrochim. Acta, Part A* **2012**, *86*, 456−460.
(17) Borghei, Y.-S.; Hosseini, M.; Khoobi, M.; Ganjali, M. R. Copper Nanocluster-Enhanced Luminol Chemiluminescence for High-Selectivity Sensing of Tryptophan and Phenylalanine. *Luminescence* **2017**, *32*, 1045−1050.
(18) Kölmel, D. K.; Kool, E. T. Oximes and Hydrazones in Bioconjugation: Mechanism and Catalysis. *Chem. Rev.* **2017**, *117*, 10358−10376.
(19) Hummel, W.; Schütte, H.; Kula, M.-R. Enzymatic Determination of L-Phenylalanine and Phenylpyruvate with L-Phenylalanine Dehydrogenase. *Anal. Biochem.* **1988**, *170*, 397−401.
(20) Wendel, U.; Hummel, W.; Langenbeck, U. Monitoring of Phenylketonuria: a Colorimetric Method for the Determination of Plasma Phenylalanine Using L-Phenylalanine Dehydrogenase. *Anal. Biochem.* **1989**, *180*, 91−94.
(21) Peschke, B.; Zundel, M.; Bak, S.; Clausen, T. R.; Blume, N.; Pedersen, A.; Zaragoza, F.; Madsen, K. C-Terminally PEGylated hGH-derivatives. *Bioorg. Med. Chem.* **2007**, *15*, 4382−4395.
(22) Harjani, J. R.; Liang, C.; Jessop, P. G. A Synthesis of Acetamidines. *J. Org. Chem.* **2011**, *76*, 1683−1691.
(23) Hermanson, G. T. *Bioconjugate Techniques*; Academic Press, 2013.
(24) Zhang, F.; Cao, L.; Yang, W. Preparation of Monodisperse and Anion-Charged Polystyrene Microspheres Stabilized with Polymerizable Sodium Styrene Sulfonate by Dispersion Polymerization. *Macromol. Chem. Phys.* **2010**, *211*, 744−751.
(25) Zhang, J.-T.; Wang, L.; Lamont, D. N.; Velankar, S. S.; Asher, S. A. Fabrication of Large-Area Two-Dimensional Colloidal Crystals. *Angew. Chem., Int. Ed.* **2012**, *51*, 6117−6120.
(26) Zhang, J.-T.; Chao, X.; Liu, X.; Asher, S. A. Two-Dimensional Array Debye Ring Diffraction Protein Recognition Sensing. *Chem. Commun.* **2013**, *49*, 6337−6339.
(27) Prevo, B. G.; Velev, O. D. Controlled, Rapid Deposition of Structured Coatings from Micro-and Nanoparticle Suspensions. *Langmuir* **2004**, *20*, 2099−2107.
(28) Dirksen, A.; Dirksen, S.; Hackeng, T. M.; Dawson, P. E. Nucleophilic Catalysis of Hydrazone Formation and Transimination: Implications for Dynamic Covalent Chemistry. *J. Am. Chem. Soc.* **2006**, *128*, 15602−15603.
(29) Dirksen, A.; Hackeng, T. M.; Dawson, P. E. Nucleophilic Catalysis of Oxime Ligation. *Angew. Chem., Int. Ed.* **2006**, *45*, 7581−7584.
(30) Crisalli, P.; Kool, E. T. Water-Soluble Organocatalysts for Hydrazone and Oxime Formation. *J. Org. Chem.* **2013**, *78*, 1184−1189.
(31) Wendeler, M.; Grinberg, L.; Wang, X.; Dawson, P. E.; Baca, M. Enhanced Catalysis of Oxime-Based Bioconjugations by Substituted Anilines. *Bioconjugate Chem.* **2013**, *25*, 93−101.
(32) Rashidian, M.; Mahmoodi, M. M.; Shah, R.; Dozier, J. K.; Wagner, C. R.; Distefano, M. D. A Highly Efficient Catalyst for Oxime Ligation and Hydrazone−Oxime Exchange Suitable for Bioconjugation. *Bioconjugate Chem.* **2013**, *24*, 333−342.
(33) Flory, P. J.; Rehner, J., Jr. Statistical Mechanics of Cross-Linked Polymer Networks I. Rubberlike Elasticity. *J. Chem. Phys.* **1943**, *11*, 512−520.
(34) Hiemenz, P. C.; Lodge, T. P. *Polymer Chemistry*; CRC Press, 2007.
(35) Bain, A. D.; Eaton, D. R.; Hamielec, A. E.; Mlekuz, M.; Sayer, B. G. Line Broadening in the Carbon-13 NMR Spectra of Cross-Linked Polymers. *Macromolecules* **1989**, *22*, 3561−3564.
(36) Shapiro, Y. E. Structure and Dynamics of Hydrogels and Organogels: An NMR Spectroscopy Approach. *Prog. Polym. Sci.* **2011**, *36*, 1184−1253.
(37) Mathur, A. M.; Scranton, A. B. Characterization of Hydrogels Using Nuclear Magnetic Resonance Spectroscopy. *Biomaterials* **1996**, *17*, 547−557.
(38) Shestakova, P.; Willem, R.; Vassileva, E. Elucidation of the Chemical and Morphological Structure of Double-Network (DN) Hydrogels by High-Resolution Magic Angle Spinning (HRMAS) NMR Spectroscopy. *Chem.—Eur. J.* **2011**, *17*, 14867−14877.

https://dx.doi.org/10.1021/acsami.0c08787
ACS Appl. Mater. Interfaces 2020, 12, 39612−39619